IEEE UKRAINE SECTION

IGOR SIKORSKY KYIV POLYTECHNIC INSTITUTE

2026 IEEE 43rd INTERNATIONAL CONFERENCE ON ELECTRONICS AND NANOTECHNOLOGY (ELNANO)

CONFERENCE PROCEEDINGS

APRIL 27-30, 2026
KYIV, UKRAINE

2026 IEEE 43rd International Conference on ELECTRONICS AND NANOTECHNOLOGY (ELNANO)

ISBN: 979-8-3315-8213-5

Online ISSN: 2693-3535

Organizing Committee of IEEE ELNANO-2026
E-mail: elnano@ieee.org.ua
Faculty of Electronics,
Igor Sikorsky Kyiv Polytechnic Institute
Building 12, Polytechnichna Street, 16/9, off. 423,
03056, Kyiv, Ukraine

Physical properties of $CdFeP_2S_6$ as a new material for spintronic devices

Henrietta Bán
Dept. of the Physics of Semiconductors
Uzhhorod National University
Uzhhorod, Ukraine
https://orcid.org/0000-0002-5635-1470

Roman Pavlyshyn
Dept. of the Physics of Semiconductors
Uzhhorod National University
Uzhhorod, Ukraine
roman.pavlyshyn@uzhnu.edu.ua

Andrew Horvat
Dept. of the Physics of Semiconductors
Uzhhorod National University
Uzhhorod, Ukraine
https://orcid.org/0000-0002-2195-6824

Anton Kohutych
Dept. of the Physics of Semiconductors
Uzhhorod National University
Uzhhorod, Ukraine
https://orcid.org/0000-0001-9138-2267

Vitaly Gerasimov
Department of Light Industry
Mukachevo State University
Mukachevo, Ukraine
https://orcid.org/0000-0001-6108-9895

Alexander Molnar
Dept. of the Physics of Semiconductors
Uzhhorod National University
Uzhhorod, Ukraine
https://orcid.org/0000-0002-3964-6170

***Abstract*— The temperature dependence of the dielectric spectra of $CdFeP_2S_6$ crystals is presented for the first time. It is shown that in the temperature range of 200-300 K, a relaxation change in the temperature-frequency dependence of the dielectric permittivity is observed. Partial replacement of Cd with Fe significantly affects the Raman spectra of $CdFeP_2S_6$ crystals compared to $Cd_2P_2S_6$.**

Keywords—$CdFeP_2S_6$, dielectric spectra, Raman spectra

I. Introduction

Maintaining the pace of modern electronics development in line with Moore's law requires moving beyond classical semiconductor circuitry. This shift involves functional elements based on diverse physical phenomena to achieve higher speed and greater component density. This applies to both characteristic dimensions (10^{-9}–10^{-10} m) and switching times (10^{-9}–10^{-10} s) of individual elements. Further gains in speed and miniaturization can be achieved by transitioning to spintronics, where both the charge and spin of electrons are used for information storage, processing, and transmission. Antiferromagnetic van der Waals materials are promising candidates for such devices. Even in the two-dimensional (2D) monolayer limit, they retain antiferromagnetic order and exhibit ultrafast spin dynamics in the THz range.

To date, a fairly large number of two-dimensional crystals of the $Me_2P_2(S,Se)_6$ family with antiferromagnetic properties are known [1,2], such as $Fe_2P_2S_6$, $CuCrP_2S_6$, $CdFeP_2Se_6$, and $CdFeP_2S_6$. Despite being synthesized in 1988 [3], this material remains relatively understudied. Only three studies on this crystal have been reported to date [3-5].

In Ref. [4], ^{57}Fe Mössbauer spectroscopy and magnetic susceptibility measurements (57–340 K) were performed on Cd-substituted $CdFeP_2S_6$. Both ferromagnetic and antiferromagnetic interactions were found to persist despite metal-ion disorder.

Reference [5] investigates the magnetic properties of layered $Fe_xCd_{1-x}PS_3$ (x=0.1÷0.8) and their methylviologen intercalates. The persistence of strong in-plane magnetic interactions, even at high dilution, indicates a non-random distribution of Fe^{2+} ions over the metal sites. The interactions are predominantly ferromagnetic at low Fe content and antiferromagnetic at higher concentrations. Ion-exchange intercalation with methylviologen strengthens the ferromagnetic coupling.

However, no data concerning the electrophysical properties of this crystal, nor any information about Raman spectra, have been found in the literature. Therefore, this work is devoted to filling in these gaps in the data on $CdFeP_2S_6$ crystals.

II. Obtaining samples

The growth of $CdFeP_2S_6$ single crystals was first reported in [3]. $CdFeP_2S_6$ were prepared in sealed quartz tubes from a stoichiometric mixture of the elements held at 600°C for a 2-week period. We used a similar method to obtain single crystals. After the synthesis period, the resulting material was slowly cooled to room temperature to prevent cracking of the samples. The result was layered black crystals (in the case of very thin plates, they were translucent dark brown) with a metallic sheen (Fig. 1), ranging in size from 5×5 mm^2 to 8×10 mm^2 and in thickness from 10 μm to 0.1 mm.

To determine the chemical composition of the samples, we used a TESCAN MIRA 3 Scanning Electron Microscope with EDAX EDS and APEX™ EDAX's premier software program for the collection and analysis of Energy Dispersive Spectroscopy (EDS) data and the compositional characterization of materials. Samples were mounted on the stage of an electron microscope using Ted Pella Double Coated Carbon Conductive Tapes. The results provided data indicating the chemical composition of the $CdFeP_2S_6$ samples (weight percentages: Cd=26.3%, Fe=13.2%, P=14.6%, S=46.0%).

According to the Materials Project database [6], theoretical calculations show that $FeCd(PS_3)_2$ crystallizes in the monoclinic *C2* space group. The structure is two-dimensional and consists of one $FeCd(PS_3)_2$ sheet oriented in the (0, 0, 1) direction. Fe^{2+} is bonded to six S^{2-} atoms to form FeS_6 octahedra that share edges with three equivalent CdS_6 octahedra.

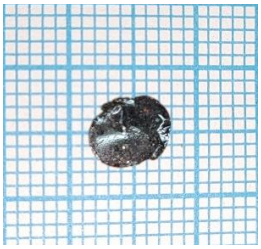

Fig. 1. Appearance of one of the $CdFeP_2S_6$ crystal samples obtained.

979-8-3315-8213-5/26/$31.00 ©2026 IEEE

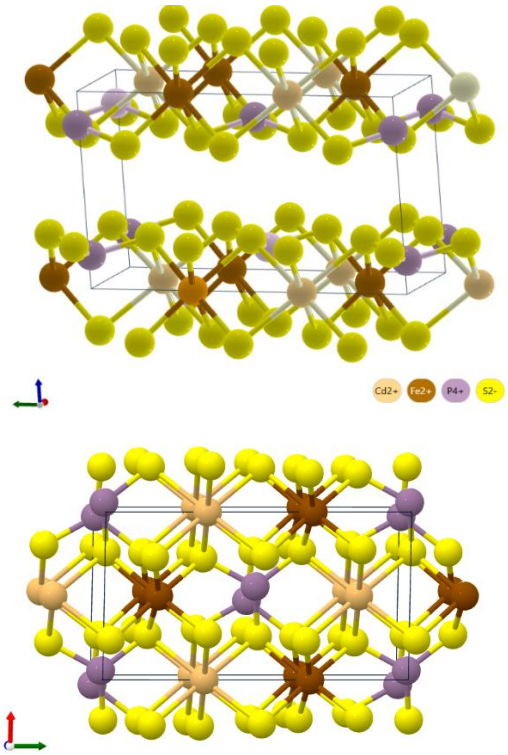

Fig. 2. Crystal structure of $CdFeP_2S_6$ according to [6].

There is a spread of Fe-S bond distances ranging from 2.46 to 2.61 Å. Cd^{2+} is bonded to six S^{2-} atoms to form CdS_6 octahedra that share edges with three equivalent FeS_6 octahedra. There are a spread of Cd-S bond distances ranging from 2.73-2.77 Å. P^{4+} is bonded in a trigonal non-coplanar geometry to three S^{2-} atoms. There is a spread of P-S bond distances ranging from 2.04 to 2.06 Å. There are three inequivalent S^{2-} sites. In the first S^{2-} site, S^{2-} is bonded in a distorted trigonal non-coplanar geometry to one Fe^{2+}, one Cd^{2+}, and one P^{4+} atom. In the second S^{2-} site, S^{2-} is bonded in a 3-coordinate geometry to one Fe^{2+}, one Cd^{2+}, and one P^{4+} atom. In the third S^{2-} site, S^{2-} is bonded in a distorted trigonal non-coplanar geometry to one Fe^{2+}, one Cd^{2+}, and one P^{4+} atom.

If we compare the data [6] with experimental works [3], the discrepancy in the lattice parameters is minimal, although the authors who first synthesized $CdFeP_2S_6$ determine its belonging to the *C2/m* space group based on X-ray structural data.

III. Experimental Setup

To study the temperature dependence of dielectric permittivity, we used an automated measuring system. All measurements were performed after annealing the samples at 400 K for 3 hours. As we established in our study of layered crystals, before any measurements of electrophysical properties, samples must be annealed to eliminate their history (illumination, natural intercalation, applied electric fields leading to ion transfer, etc.). This process "resets" the sample's history and ensures good repeatability of results.

For our research, we used several samples ranging in size from 5×5×0.01 mm^3 to 6×8×0.1 mm^3. Electrodes made of conductive silver paste were applied to the surface of the crystals. To check the effect of the electrodes, several samples were studied using carbon powder electrodes, but no difference in the data obtained was observed compared to the silver electrodes. To bring the experiments to the same conditions, the intensity of the measuring field was always adjusted for different samples, taking into account their thickness.

A. Dielectric measurement

To measure the dielectric constant, an LCR GW Instek LCR-819 meter with a frequency range of 12 Hz - 100 kHz and a measuring voltage of 50 mV - 1.25 V was chosen.

Because layered $Me_2P_2(S,Se)_6$ crystals often exhibit ionic conductivity, measurements were performed at a low applied voltage of 50 mV. This minimizes ionic contributions and reduces dielectric nonlinearity caused by high electric fields in thin samples.

The use of a small amplitude of the measuring field led to a fairly large scatter of the measured parameters, especially at low frequencies, so the measurement speed was set to the minimum - one measurement per second. The measurement accuracy was 0.05%.

B. Raman spectra measurement

To study the Raman spectra, we used the XploRA PLUS System spectrometer from HORIBA Scientific. The spectra were obtained at a wavelength of 532 nm, over 3 seconds, averaging was made over 20 measurements, using a density filter of 1% and in two polarization configurations of 0° and 45°.

C. Temperature measurement

Measurements of temperature dependences were carried out using an automated computer-controlled system in an immersion-type cryostat based on a Measurement Computing USB-TEMP-AI data acquisition device and a Linear Programmable DC Power Supply, OWON ODP3033, which allows us to change the heating and cooling rate in the range of 0.001 K/min to 1 K/min. As a temperature sensor, the PT100/1509A platinum thermistor of TDI Ltd. (England) was applied. The temperature measurement resolution was 0.001 K, with an absolute accuracy of ± 2.9 K at 73 K and 0.27 K at 373 K.

IV. Dielectric Spectra

Dielectric spectra of $CdFeP_2S_6$ single crystals were measured between 80 and 400 K. The results indicate a relaxation-type temperature–frequency behavior of the dielectric response. The maximum anomaly of the imaginary part ε" and the corresponding break in the real component ε' of the complex dielectric permittivity, as shown in Fig. 3, occurs at a temperature of 250 K at a frequency of 10 kHz.

Interestingly, similar behavior is observed in both bulk $Sn_2P_2S_6$ crystals [7], layered $CuInP_2S_6$ crystals [8] and solid solutions $Cu_{0.3}Fe_{3.4}P_2S_6$ [9]. However, in the case of $Sn_2P_2S_6$ (which is a ferroelectric), this relaxation behavior is explained by the dynamics of small hole polarons with donor-acceptor compensation processes in the crystal lattice with tin and sulfur vacancies [7].

In the case of $Cu_{0.3}Fe_{3.4}P_2S_6$ mixed materials, similar behavior can be explained by Maxwell-Wagner relaxation occurring at the boundaries between crystallites and inter-crystallite boundaries [9].

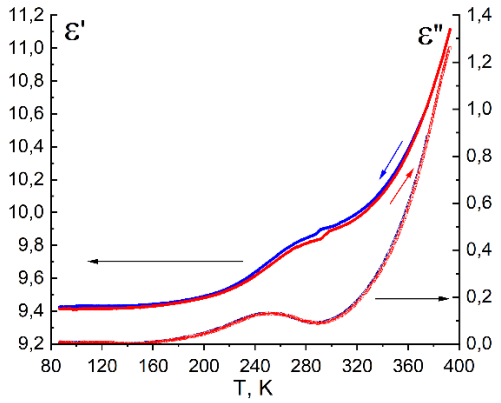

Fig. 3. Temperature dependence of the real ε', and imaginary ε" parts of the complex permittivity $\varepsilon^* = \varepsilon' - i\varepsilon''$ of the $CdFeP_2S_6$ crystal.

In the case of $CuInP_2S_6$ crystals (which are also ferrielectric), low-temperature anomalies of a similar nature are interpreted as behavior characteristic of dipole glass [8].

Such a wide range of interpretations is rather strange for materials belonging to the same $Me_2P_2S_6$ group, in which only the $[P_2S_6]^{4-}$ anion is a common component of these compounds.

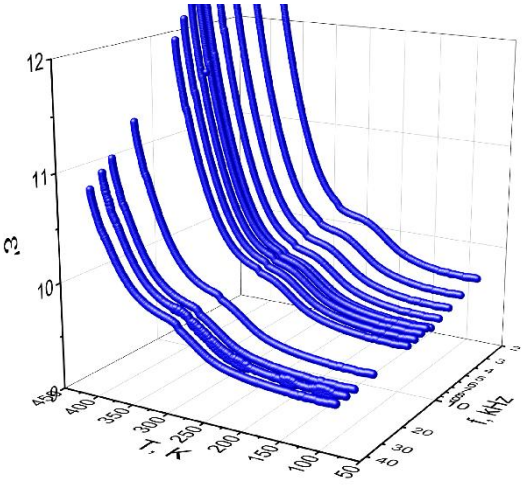

(a)

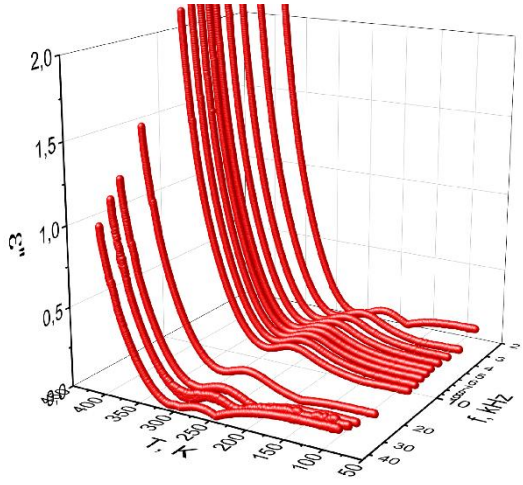

(b)

Fig. 4. Temperature-frequency dependence of the real – (a), and imaginary – (b), parts of the complex permittivity $\varepsilon^* = \varepsilon' - i\varepsilon''$ of the $CdFeP_2S_6$ crystal

Figure 4 show the temperature dependence of the real ε' – (a) and imaginary ε" – (b) components of the complex permittivity ε^*. tg $\delta_{300K} \approx 0.01$ at $f = 10$ kHz.

The observed dielectric spectra (see Fig. 5) can be described by the Cole-Cole formula [10]

$$\varepsilon^* = \varepsilon_\infty + \frac{\Delta\varepsilon}{1 + (i\omega\tau)^{1-\alpha}}$$

where Δε is the dielectric relaxation force, τ is the average and most probable Cole-Cole relaxation time, ε_∞ is the contribution of all polar phonons and electron polarization to the dielectric permittivity, $0 \le \alpha \le 1$ is the width parameter of the Cole-Cole distribution functions. At α = 0 this equation reduces to Debye's formula. In our case $\Delta\varepsilon \approx 0.5$, and $\tau \approx 2\times10^{-4}$ s. The distribution parameter of relaxation times α is very high ($\alpha \gtrsim 0.4$–0.6) and decreases with cooling, indicating a very large distribution of relaxation times.

For maximum relaxation losses ε", the condition $\omega\tau(T_{max}) \approx 1$ is satisfied, where $\omega = \pi f$. The temperature dependence of the relaxation time is usually described by the Arrhenius law:

$$f(T) = f_0 exp\left(-\frac{E_a}{k_B T_{max}}\right),$$

where $k_B \approx 8.617333\times10^{-5}$ eV/K, f_0 is the frequency to which $T_{max} \to \infty$ approaches, and the activation energy E_a is defined as

$$E_a = k_B T_{max} ln\left(\frac{f_0}{f}\right).$$

In our case, $f_0 \approx 10^{11}$ Hz (which coincides well with the data from [10]), and the activation energy of this process is $E_a \approx 0.347$ eV.

In the high-temperature range (see Fig. 4(b)), above 300 K, the sharp increase in the imaginary part of the dielectric permittivity ε" (dielectric losses), as in the case of most semiconductor materials of the $Me_2P_2S_6$ family, is caused by the increase in the electrical conductivity of the samples with increasing temperature, which accordingly contributes to the real component of the dielectric permittivity. These two processes—temperature activation of conductivity and relaxation mechanism in the 200–300 K range—overlap, as can be seen in Figure 4(a).

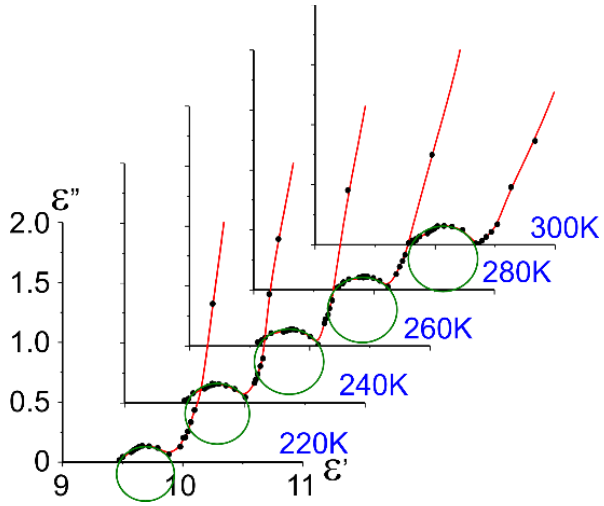

Fig. 5. Cole-Cole diagrams constructed at different temperatures.

In the high-temperature range (see Fig. 4(b)), above 300 K, the sharp increase in the imaginary part of the dielectric permittivity ε" (dielectric losses), as in the case of most semiconductor materials of the $Me_2P_2S_6$ family, is caused by the increase in the electrical conductivity of the samples with increasing temperature, which accordingly contributes to the real component of the dielectric permittivity. These two processes—temperature activation of conductivity and relaxation mechanism in the 200–300 K range—overlap, as can be seen in Figure 4(a).

It is also interesting to note a small break in the temperature dependence of the dielectric permittivity at a temperature of ≈290 K (Fig. 3 and Fig. 4(a)). Such behavior is characteristic of structural phase transitions observed, for example, in the $Cd_2P_2S_6$ crystal at a lower temperature of ≈228 K [11]. This break is present on both the cooling and heating curves, with a hysteresis of about 5 K. Further, preferably structural, studies are needed to clarify the nature of this anomaly.

V. Raman spectra

We obtained Raman spectra of $CdFeP_2S_6$ crystals at a wavelength of 532. Since these spectra were obtained for the first time and have not yet been clearly interpreted, we compared them with Raman spectra of more-studied $Cd_2P_2S_6$ crystals at room temperature.

The comparison results are shown in Fig. 6. For greater clarity, the spectra are normalized according to the intensity of the P-P Raman line at 374 cm^{-1}.

According to data [12], the lines at 80 and 125 cm^{-1} are caused by translational vibrations of Cd^{2+} ions. When Cd is replaced by Fe in the spectra shown in Fig. 7, we indeed observe a significant change in both the shape and amplitude of the corresponding Raman lines. 221, 247 and 270 cm^{-1} S-P-S phonon modes originating from the symmetry of P_2S_6 units are also common in compounds of the MPS_3 family. Partial replacement of Cd with Fe also significantly affects these fluctuations. 377 cm^{-1} is dominated by out-of-plane P-P and S valence vibrations (PS_3 stretching mode). 562 cm^{-1} was caused by the out-of-plane P-S valence vibrations.

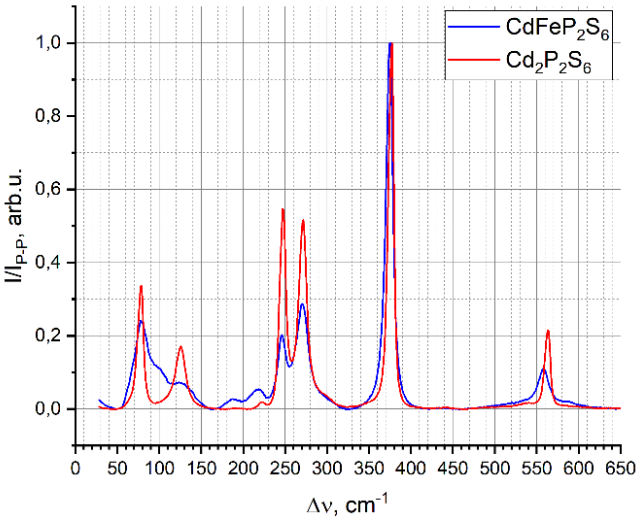

Fig. 6. Comparison of Raman spectra of $Cd_2P_2S_6$ and $CdFeP_2S_6$ crystals obtained at a wavelength of 532 nm.

VI. Conclusions

Based on the obtained data, $CdFeP_2S_6$ crystals exhibit relaxation behavior in the temperature–frequency dependence of the dielectric permittivity in the 200–300 K temperature range. At 290 K, an anomaly in ε′(T) is observed, resembling the structural phase transition reported for $Cd_2P_2S_6$ at lower temperatures. The dielectric permittivity of $CdFeP_2S_6$ is comparable to that of $Cd_2P_2S_6$ and significantly lower than that of the ferroelectrics $Sn_2P_2S_6$ and $CuInP_2S_6$. This behavior is expected, as $CdFeP_2S_6$ does not contain polar dipoles that would strongly contribute to the dielectric response. Partial substitution of Cd by Fe results in a pronounced rearrangement of the Raman scattering spectra, particularly in the low-frequency region below 150 cm^{-1}. Additional changes are observed in the 220–300 cm^{-1} range, associated with S–P–S phonon modes, which are also strongly influenced by the cationic sublattice.

Acknowledgement

This work was partly funded by the HORIZON Project ID: 101131229 "2D Piezo" and the Ministry of Education and Science of Ukraine under project 0125U001555 "Low-dimensional chalcogen phosphates for nanoenergy and highly integrated heterostructures".

References

[1] K.S. Burch, D. Mandrus, J.G. Park, "Magnetism in two-dimensional van der Waals materials", Nature, vol.563, pp.47–52, 01 November 2018, DOI: 10.1038/s41586-018-0631-z

[2] S. Rahman, J.F. Torres, A.R. Khan, Y. Lu, "Recent Developments in van der Waals Antiferromagnetic 2D Materials: Synthesis, Characterization, and Device Implementation", ACS Nano, vol.15, pp.17175−17213, 2021, DOI: 10.1021/acsnano.1c06864

[3] S. Lee, P. Colombet, G. Ouvrard, R. Brec, "General Trends Observed in the Substituted Thiophosphate Family. Synthesis and Structure of $AgScP_2S_6$ and $CdFeP_2S_6$", Inorg. Chem., vol.27, pp.1291-1294, 1988, DOI: 10.1021/ic00280a041

[4] A. Bhomwick, B. Bal, S. Ganguly, M. Bhattacharya, M.L. Kundu, "Investigation of the layered compound $Fe_{0.5}Cd0.5PS_3$", J. Phys. Chem. Solidv, Vol.53, No. 10, pp.1279-1284, 1992, DOI: 10.1016/0022-3697(92)90246-A

[5] A. Le´austic, E. Rivie`re, R. Cle´ment, E. Manova, I. Mitov, "Investigation of the Influence of Intercalation on the Magnetic Properties of $Fe_xCd_{1-x}PS_3$ Layered Compounds", J. Phys. Chem. B, vol.103, pp.4833-4838, 1999, DOI: 10.1021/jp9904623

[6] [Online] Available: https://next-gen.materialsproject.org/materials/mp-1226823?formula=CdFe%28PS3%292. Accessed at 03.12.2025.

[7] H. Ban, D. Gal, A. Kohutych, A. Molnar, "Low-temperature anomalies of the dielectric permeability of $Sn_2P_2S_6$ crystals", Low Temp. Phys., vol. 50, №1, pp.56-65, 2024, DOI: 10.1063/10.0023893

[8] J. Banys, A. Dziaugys, K. E. Glukhov, A. N. Morozovska, N. V. Morozovsky, Yu. M. Vysochanskii, "Van der Waals ferroelectrics. Properties and device applications of phosphorous chalcogenides", Wiley-VCH GmbH, 2021, 400 p. ISBN 978-3-527-35034-6

[9] A. Dziaugys, J. Macutkevic, S. Svirskas, R. Juskenas, M. Wencka, J. Banys, S.F. Motria, Yu. Vysochanskii, "MaxwelleWagner relaxation and anomalies of physical properties in $Cu_{0.15}Fe_{1.7}PS_3$ mixed material", Journal of Alloys and Compounds, vol.650, pp.386-392, 2015, DOI: 10.1016/j.jallcom.2015.07.261

[10] K. S. Cole, R. H. Cole, "Dispersion and Absorption in Dielectrics I. Alternating Current Characteristics", J. Chem. Phys. vol. 9, I. 4, pp. 341–351, 1 April 1941, DOI: 10.1063/1.1750906

[11] H. Ban, D. Gal, S. Motrja, A. Molnar, "Hysteresis phenomena in $Cd_2P_2S_6$ layered crystals", Low Temperature Physics, vol. 51, № 1, pp. 53–58, 2025, DOI: 10.1063/10.0034644

[12] S. Rahman, H. Ngyuen, D. Macdonald, Y. Lu, "Temperature-Dependent Phase Variations in Van Der Waals $CdPS_3$ Revealed by Raman Spectroscopy", Symmetry, vol.16(2), pp.140-153, 24 January 2024, DOI: 10.3390/sym16020140